Research Paper

Thrombin induces striatal neurotoxicity depending on mitogen-activated protein kinase pathways *in vivo*

Shinji Fujimoto, Hiroshi Katsuki, Masatoshi Ohnishi, Mikako Takagi, Toshiaki Kume, Akinori Akaike

Department of Pharmacology, Graduate School of Pharmaceutical Sciences, Kyoto University, 46-29 Yoshida-shimoadachi-cho, Sakyo-ku, Kyoto 606-8501, Japan.

Address correspondence to Akinori Akaike, Ph.D.

Department of Pharmacology,

Graduate School of Pharmaceutical Sciences, Kyoto University

46-29 Yoshida-shimoadachi-cho, Sakyo-ku, Kyoto 606-8501, Japan.

Phone: +81-75-753-4550 FAX: +81-75-753-4579

E-mail: aakaike@pharm.kyoto-u.ac.jp

Appropriate Section Editor: Dr. Yoland Smith (Neuropharmacology)

Abbreviations

EGTA; ethyleneglycol bis(2-aminoethylether)tetraacetic acid, ERK; extracellular signal regulated kinase, ICH; intracerebral hemorrhage, iNOS; inducible nitric oxide synthase, i.p.; intraperitoneal injection, JNK; c-Jun *N*-terminal kinase, MAPK; mitogen-activated protein kinase, NeuN; neuronal nuclei, o.d.; outer diameter, PBS; phosphate buffered saline, SDS; sodium dodecyl sulfate, SEM; standard error of mean, Tris; tris(hydroxymethyl)aminomethane.

Abstract

Intracerebral hemorrhage represents stroke characterized by formation and expansion of hematoma within brain parenchyma. Blood-derived factors released from hematoma are considered to be involved in poor prognosis of this disorder. We previously reported that thrombin, a blood-derived serine protease, induced cytotoxicity in the cerebral cortex and the striatum in organotypic slice cultures, which depended on mitogen-activated protein kinase (MAPK) pathways. Here we investigated the mechanisms of thrombin cytotoxicity in the striatum *in vivo*. Thrombin microinjected into the striatum of adult rats induced neuronal death and microglial activation around the injection site. Neuronal loss without any sign of nuclear fragmentation was observed as early as 4 h after thrombin injection, which was followed by gradual neuronal death exhibiting nuclear fragmentation. Thrombin-induced damage assessed at 72 h after injection was partially but significanty reduced by concomitant administration of inhibitors of MAPK pathways. Activation of extracellular signal-regulated kinase (ERK) and p38 MAPK in response to thrombin was verified by western blot analysis. Moreover, phosphorylated ERK and p38 MAPK were localized prominently in reactive microglia, and inhibition of microglial activation by minocycline attenuated thrombin-induced damage, suggesting that reactive microglia were responsible for thrombin-induced neuronal death. Thus, MAPK pathways and microglial activation may serve as therapeutic targets of pathogenic conditions associated with hemorrhagic stroke.

Keywords: apoptosis, intracerebral hemorrhage, microglia, microinjection, striatum

Intracerebral hemorrhage (ICH) represents approximately 15% of all strokes. Undesirable prognosis due to the lack of efficient therapeutic interventions makes ICH a serious clinical problem (Fayad and Awad, 1998). Ganglionic hemorrhages are the most common forms of ICH, followed by lobar ones (Xi et al., 2006). While physical trauma and mass effect could participate in brain damage after hemorrhagic events (Sinar et al., 1987), accumulating evidence demonstrates that brain edema after ICH is caused by hematoma-derived components (Huang et al., 2002; Sansing, et al., 2003) including thrombin (Lee et al., 1996; Kitaoka et al., 2002).

Thrombin is a blood-derived serine protease essential to coagulation and is abundantly present in hematoma. Uncontrolled thrombin activity after ICH could cause neuronal cell death as well as brain edema. For example, evidence has shown that thrombin induces cell death with characteristics of apoptosis in cultured neurons and astrocytes (Donovan et al., 1997) and that intrastriatal injection of thrombin increases apoptotic cells and causes brain damage (Xue and Del Bigio, 2001). Moreover, *in vitro* and *in vivo* studies have demonstrated that thrombin activates microglial cells in the midbrain, thereby causing dopaminergic neuronal death (Choi et al., 2003; Katsuki et al., 2006).

Despite increasing amount of information on thrombin and ICH, few studies have addressed the mechanisms of neuronal damage after ICH in the striatum. In this context, we have previously reported that thrombin induces shrinkage of the striatal tissue in organotypic cortico-striatal slice cultures. The tissue shrinkage was dependent on activation of microglia and mitogen-activated protein kinase (MAPK) pathways (Fujimoto et al., 2006). Based on these findings, here we examined the mechanisms of cytotoxicity of thrombin microinjected into the striatum of adult rats, with special reference to microglia and MAPKs.

Experimental procedures

Drugs and chemicals

Drugs and chemicals were obtained from Nacalai Tesque (Kyoto, Japan), unless otherwise indicated. Thrombin from bovine plasma (catalog No. T4648 and T3399), bovine serum albumin (catalog No. A2153) and minocycline hydrochloride were obtained from Sigma (St. Louis, MO, USA). Argatroban was from Sawai Pharmaceutical (Osaka, Japan). PD98059 and SB203580 were from Calbiochem (San Diego, CA, USA). SP600125 was from Tocris Cookson (Bristol, UK).

Surgical procedures and drug administration

Male Sprague-Dawley rats initially weighing 220 - 280 g were used. Animals were kept at constant ambient temperature (24 ± 1 °C) under a 12-h light and dark cycle with free access to food and water. Experiments were conducted in accordance with the ethical guidelines of Kyoto University animal experimentation committee, and the guidelines of the Japanese Pharmacological Society. Drug administration was performed according to a previous report (Xue and Del Bigio, 2001) with modification. Briefly, rats were anesthetized with pentobarbital (50 mg/kg, i.p., Dainippon Sumitomo Pharmaceutical, Osaka, Japan) and placed in a stereotaxic frame (Narishige, Tokyo, Japan). After scalp incision, a hole was drilled on the skull. For intrastriatal injection, each rat was unilaterally implanted with a stainless steel guide cannula (o.d. 0.7 mm) above the right striatum (0.2 mm anterior, 3.0 mm lateral from bregma). The guide cannula was held firmly in place by dental acrylic cement (Nisshin Dental Products Inc., Kyoto, Japan). Drugs were administered via a stainless steel injection cannula (o.d. 0.35 mm), whose tip was inserted 6.0 mm below the surface of the skull. Drug

solution in a volume of 5 μl/rat was infused at a constant rate of 0.5 μl/min. Unless otherwise indicated, thrombin (catalog No. T4648, Lot 023K7602, 24.5 U/mg solid) dissolved in saline at 4000 U/ml (163 mg/ml) was used, where thrombin activity was expressed by NIH units. The injection cannula was left in place for at least additional 5 min to prevent backflow of drugs. Minocycline was given intraperitoneally at a dose of 45 mg/kg at 1 and 13 h after thrombin injection, and at 22.5 mg/kg at 25, 37 and 49 h. These doses approximate those used in a study on experimental intracerebral hemorrhage (Power et al., 2003). Control rats received intraperitoneal injection of the equivalent volume of saline.

Histological examination

After indicated periods from intrastriatal injection, rats were anesthetized again and perfused through the heart with phosphate buffered saline (PBS) followed by 4% paraformaldehyde. Brains were removed and postfixed in 4% paraformaldehyde and dehydrated with 15% sucrose solution for overnight at 4°C. After freezing, coronal brain sections (16 μm) containing the injection site were prepared and mounted onto slides. They were then subjected to nuclear staining or to immunohistochemistry. Cell nuclei were stained with Hoechst 33342 (0.1 mg/ml, Molecular Probes, Eugene, OR, USA) for 1 h at room temperature and visualized by ultraviolet illumination. For immunohistochemitry, specimens were autoclaved (121°C for 15 min) for epitope retrieval. After rinse with PBS, they were permeabilized and blocked with 0.5% Triton X-100 in PBS containing 1.5% horse serum or goat serum for 1 h at room temperature. Specimens were then incubated with primary antibodies overnight at 4°C. Primary antibodies were mouse anti-NeuN (1:200, Chemicon International, Temecula, CA, USA), mouse anti-OX42 (1:300, Dainippon

Pharmaceutical, Osaka, Japan), rabbit anti-phospho-p44/42 MAP kinase (T202/Y204) (1:250, Cell Signaling Technology, Beverly, MA, USA), rabbit anti-phospho-p38 MAP kinase (T180/Y182) (1:250, Cell Signaling Technology) and rabbit anti-iNOS (1:250, BD Transduction Laboratories, San Diego, CA, USA). For immunohistochemistry with anti-OX42 antibody, epitope retrieval was not performed. After rinse with PBS, specimens were incubated with secondary antibodies for 1 h at room temperature. Alexa Fluor 568-labeled goat anti-rabbit IgG (1:200, Molecular Probes), Alexa Fluor 488-labeled goat anti-mouse IgG (1:200, Molecular Probes) and biotinylated horse anti-mouse IgG (1:200, Vector Laboratories, Burlingame, CA, USA) were used as secondary antibodies. After incubation with the biotinylated secondary antibody, specimens were treated with avidin-biotinylated horseradish peroxidase complex (Vectastain Elite ABC kit, Vector Laboratories), and then peroxidase was visualized with 0.07% diaminobenzidine and 0.018% H_2O_2. Bright-field images were captured through a monochrome chilled CCD camera (C5985; Hamamatsu Photonics, Hamamatsu, Japan) and stored as image files. We defined the striatal region without NeuN-positive cells as the injured region, and measured the injured area with NIH Image 1.63. Fluorescence signals were observed with a laser-scanning confocal microscopic system (MRC1024, Biorad, Hercules, CA, USA).

Western blot analysis

After indicated periods from thrombin injection, the striatal tissue including the injection site was harvested and homogenized in ice-cold lysis buffer containing 20 mM Tris–HCl (pH 7.0), 25 mM β-glycerophosphate (Sigma), 2 mM EGTA•2Na, 1% Triton X-100, 1 mM vanadate, 1% aprotinin (Sigma), 1 mM phenylmethylsulfonyl fluoride and 2 mM

dithiothreitol. The contralateral striatum was also harvested as a control in several experiments. Samples were mixed with a sample buffer composed of 124 mM Tris–HCl (pH 6.8), 4% sodium dodecyl sulfate (SDS), 10% glycerol, 0.02% bromophenol blue and 4% 2-mercaptoethanol. After boiling for 5 min, samples were subjected to 12% SDS-polyacrylamide gel electrophoresis for 70 min, followed by transfer to PVDF membrane (Millipore, Bedford, MA, USA) for 70 min. Membranes were blocked for at least 1 h by 5% nonfat milk at room temperature and subsequently incubated overnight with mouse anti-phospho-p44/42 MAP kinase (T202/Y204) (1:2000, Cell Signaling Technology), rabbit anti-p44/42 MAP kinase (1:1000, Cell Signaling Technology), rabbit anti-phospho-p38 MAP kinase (1:500, Cell Signaling Technology), rabbit anti-p38 MAP kinase (1:1000, Cell Signaling Technology) and mouse anti-β-actin (1:50000, Sigma). The membranes were rinsed and incubated with horseradish peroxidase-conjugated goat anti-mouse IgG (1:10000, Jackson Immunoresearch Laboratories, West Grove, PA, USA) and goat anti-rabbit IgG (1:10000, Jackson Immunoresearch Laboratories). After incubation with secondary antibodies, membranes were rinsed and bound antibodies were detected with enhanced chemiluminescence kit (Amersham Biosciences, Buckinghamshire, UK) according to the manufacturer's instructions. The band intensities were analyzed with NIH image 1.63.

Statistics

Data are expressed as means ± SEM. Statistical significance of difference was evaluated with Student *t*-test, or with one-way analysis of variance followed by Student–Newman–Keuls' test for multiple comparisons. Probability values less than 5% were considered significant.

Results

Thrombin induces striatal neuronal death and microglial activation

We injected thrombin into the right striatum of adult rats and examined brain sections immunostained with anti-NeuN antibody (Fig. 1). The number of neurons around the injection site started to decrease 4 h after thrombin injection (Fig. 1D and E). Thereafter, the number of neurons progressively decreased and only few neurons were alive after 72 h of thrombin injection (Fig. 1K and M). To visualize morphology of cell nuclei, several brain sections were stained with Hoechst 33342. At 4 h after thrombin injection, cell nuclei around the injection site exhibited no sign of nuclear fragmentation (Fig. 1F). In contrast, several fragmented nuclei were found after 24 h and 72 h of thrombin injection in areas peripheral to the injection site (Fig. 1I andL). Immunohistochemistry on brain sections obtained after 72 h of thrombin injection revealed that there were very few NeuN-positive cells around the injection site, and we could easily distinguish the border between regions with or without NeuN immunoreactivity (Fig. 1J). Accordingly, we evaluated the degree of cytotoxicity by the injured area defined as a region without NeuN immunoreactivity in the striatum. Administration of 20 U thrombin (Sigma, catalog No. T4648, Lot 023K7602, 24.5 U/mg solid) resulted in 3.44 ± 0.25 mm^2 of injured area at 72 h (n=8). Another thrombin preparation (Sigma, catalog No. T3399, Lot 045K7590, 51 U/mg solid) given at the same dose (20 U) induced a similar degree of injury (3.52 ± 0.29 mm^2 of injured area at 72 h, n=4). In contrast, we did not observe changes in NeuN immunoreactivity or nuclear morphology when we injected bovine serum albumin at a concentration of the protein equivalent to thrombin T4648 solution (0.816 mg in 5 μl saline, data not shown). In addition, argatroban (2.5 μg mixed in thrombin solution), a thrombin inhibitor, significantly reduced thrombin

toxicity (2.43 ± 0.28 mm^2 of injured area, n=8; P=0.017 vs. thrombin T4648 alone). These results suggest that thrombin induces necrotic neuronal death shortly after injection, as well as delayed apoptotic neuronal degeneration.

Contrary to the loss of NeuN immunoreactivity, thrombin injection caused drastic augmentation of immunoreactivity for OX42, a marker protein of microglia. At the injection site, microglia changed their morphology from ramified shape into activated amoeboid shape at 4 h after thrombin injection. At 72 h, thrombin-injected striatum was occupied by a markedly increased number of activated microglia, whereas microglia retained their population and ramified appearance in the contralateral striatum (Fig. 2B-D). Some but fewer microglia showing amoeboid morphology were observed in the saline-injected striatum, which probably resulted from mechanical damage caused by needle insertion (Fig. 2A). Nevertheless, the number of activated microglia in thrombin-injected striatum increased approximately 10 times larger than that in saline-injected striatum (3374 ± 408 vs. 312 ± 40 cells/section, n=4 for each condition, P=0.005). These results suggest that thrombin induces microglial proliferation and activation in the striatum.

MAPKs are involved in thrombin-induced striatal neuronal death

We previously showed that inhibition of MAPK pathways perturbed thrombin-induced striatal shrinkage in organotypic slice cultures (Fujimoto et al., 2006). Therefore we examined the effects of inhibitors of MAPK pathways on thrombin cytotoxicity *in vivo*. We used PD98059 (5 nmol), a MAPK kinase inhibitor, SB203580 (5 nmol), a p38 MAPK inhibitor, and SP600125 (5 nmol), a c-Jun *N*-terminal kinase (JNK) inhibitor. Vehicle (saline with DMSO as solvent) or MAPK inhibitors were mixed with thrombin solution and the

mixture was injected into the striatum. We found that all of these inhibitors were neuroprotective against thrombin cytotoxicity. The protective effects were manifested by significant reduction of the injured area (Fig. 3). A clear border between the injured area and the intact area was observed also in the striatum treated with thrombin plus MAP kinase inhibitors, and MAPK inhibitors did not increase the number of NeuN-positive cells within the injured area. The density of NeuN-positive cells in the contralateral striatum in the brain section prepared from thrombin-injected rats was 1172 ± 33 cells/mm^2 (n=9), and thrombin-induced decrease of NeuN immunoreactivity corresponded to the loss of 4330 ± 321 neurons/section. Likewise, the numbers of NeuN-positive cells lost after treatment with thrombin plus PD98059, SB203580 and SP600125 were estimated to be 3492 ± 239 (n=9), 3220 ± 209 (n=8) and 3451 ± 223 (n=8) cells/mm^2, respectively, all of which were significantly smaller ($P<0.05$) than that after treatment with thrombin.

To further clarify the involvement of MAPK pathways, we examined the phosphorylation level of MAPKs by western blot analysis. Phosphorylated extracellular signal regulated kinase (ERK) increased promptly after thrombin injection and declined thereafter, whereas phosphorylated p38 MAPK increased gradually, which was accompanied by an increase in total p38 MAPK (Fig. 4A-C). To determine cell types exhibiting ERK phosphorylation after 4 h of thrombin injection, we performed double immunofluorescence with combination of antibodies against phosphorylated ERK and cell type-specific marker proteins. Immunostaining revealed that most of phosphorylated ERK-positive cells were microglia (Fig. 4D). We also tried to identify cells that express phosphorylated p38 MAPK in brain sections obtained after 72 h of thrombin injection. As shown in Fig. 4E, phosphorylated p38 MAPK also colocalized with OX42, a marker of microglia.

We further examined the involvement of reactive microglia in thrombin neurotoxicity. After thrombin injection into the striatum, minocycline, an inhibitor of microglial activation (Power et al., 2003), or saline was intraperitoneally administered. Minocycline treatment significantly reduced the number of reactive microglia around the injection site (Fig. 5A) and the injured area (Fig. 5B). Moreover, double immunofluorescence with antibodies against inducible nitric oxide synthase (iNOS) and OX42 revealed that some reactive microglia expressed iNOS after 24 h of thrombin injection in the ipsilateral striatum but not in the contralateral side (Fig. 5C, D). These results suggest that reactive microglia are responsible for thrombin neurotoxicity.

Discussion

Thrombin induces neuronal loss *in vitro* (Donovan et al., 1997; Katsuki et al., 2006) and *in vivo* (Xue and Del Bigio, 2001; Choi et al., 2003). The detrimental effects of thrombin are considered to be one of the major causes of ICH-induced neurologic deficits (Gingrich and Traynelis, 2000; Xi et al., 2003). Thus the regulation of thrombin cytotoxicity could have a therapeutic potential for ICH (Kitaoka et al., 2002). In previous work on cortico-striatal slice cultures, we demonstrated that thrombin induces apoptotic neuronal death with a long delay (Fujimoto et al., 2006). Here we investigated whether delayed apoptotic neuronal death occurs in adult rat striatum in response to thrombin. Predictably, thrombin induced neuronal loss around the injection site in the striatum. Two thrombin preparations with different purities induced a similar degree of injury when administered at the same dosage of total activity. In addition, thrombin toxicity was significantly attenuated by a thrombin inhibitor, argatroban. Previous results *in vitro* also showed that cytotoxicity of thrombin in the striatal tissue was blocked by prior heat-inactivation or by co-application of argatroban (Fujimoto et al., 2006). Overall, our observations indicate that proteolytic activity contributes to the neurotoxicity of thrombin in the striatum, although the involvement of non-proteolytic potential of thrombin preparation could not be entirely ruled out (Weinstein et al., 2005).

Unexpectedly, thrombin reduced the number of NeuN-positive cells around the injection site as early as 4 h of injection. This acute loss of neurons may result from necrotic death of some neuronal populations (Xue and Del Bigio, 2001), because we did not observe any cell nuclei undergoing fragmentation at 4 h after thrombin injection. On the other hand, many fragmented nuclei were observed at 1 or 3 days after thrombin injection, suggesting that the

loss of NeuN-positive cells in later days is a consequence of apoptotic neuronal death. Consistent with our observations, a previous report has demonstrated that apoptotic cells do not increase at 6 h after thrombin infusion (Gong et al., 2001). Our results are also in agreement with the time window of delayed thrombin- and ICH-induced apoptosis (Matsushita et al., 2000; Gong et al., 2001; Xue and Del Bigio, 2001). We did not examine the effect of caspase inhibitors against thrombin neurotoxicity, because we found previously that a caspase-3 inhibitor had no effect on thrombin cytotoxicity in cortico-striatal slice cultures (Fujimoto et al., 2006).

In the present study, phosphorylation of ERK was found in the ipsilateral striatum at 4 h after thrombin injection. Prompt ERK phosphorylation is consistent with our previous findings *in vitro* (Fujimoto et al., 2006; Katsuki et al., 2006). In addition, blockade of ERK pathway by PD98059 could reduce thrombin-induced loss of neurons, as reflected by the decrease in the injured area. These results suggest that ERK pathway participates in thrombin neurotoxicity in the striatum. We also detected a gradual increase in the level of phosphorylated p38 MAPK after thrombin injection. Interestingly, however, phosphorylation of p38 MAPK was accompanied by elevation of total p38 MAPK protein level. It is thus plausible that elevated level of phosphorylated p38 MAPK was a consequence of an increase in p38 MAPK itself. Nevertheless, inhibition of p38 MAPK by SB203580 decreased thrombin-induced injury, indicating that p38 MAPK pathway is also involved in thrombin-induced neuronal death in the striatum. Together with the protective effect of a JNK inhibitor SP600125, our present results demonstrated that ERK, p38 MAPK and JNK are all involved in thrombin-induced striatal damage *in vivo*. These observations are consistent with our previous findings *in vitro* that PD98059, SB203580 and SP600125 all

suppressed thrombin-induced shrinkage of the striatal tissue in organotypic culture (Fujimoto et al., 2006). PD98059 and SB203580 were also shown to attenuate thrombin-induced dopaminergic neuronal death in the midbrain *in vivo* (Choi et al., 2003). On the other hand, SP600125 exacerbates, and SB203580 shows no effect on, thrombin-induced cortical injury *in vitro* (Fujimoto et al., 2006), suggesting differential involvement of MAPKs in the regulation of thrombin neurotoxicity between the cerebral cortex and the striatum. Whether cortical injury induced by thrombin *in vivo* is regulated by MAPKs in a similar way to that *in vitro* remains to be determined.

Participation of reactive microglia in thrombin neurotoxicity has been reported in several studies (Choi et al., 2003; Katsuki et al., 2006). Here we observed reactive microglia characterized by strong OX42 immunoreactivity with amoeboid appearance after thrombin injection. Phosphorylation of ERK and p38 MAPK in these reactive microglia was also visible, which may be related to the detrimental effects of thrombin (Koistinaho and Koistinaho, 2002). Moreover, thrombin-induced neuronal injury was reduced by administration of minocycline, an inhibitor of microglial activation (Power et al., 2003), consistent with deleterious actions of reactive microglia. A plausible mechanism of the involvement of reactive microglia in neurotoxicity is that these cells may release cytokines and nitric oxide (Möller et al., 2000), which results from activation of NF-κB as a consequence of activation of MAPK pathways (Ryu et al., 2000; Suo et al., 2003). Indeed, we demonstrated here that a subpopulation of reactive microglia in the striatum expressed iNOS after thrombin injection. Whether nitric oxide production participates in the striatal neurotoxicity of thrombin *in vivo* remains to be determined, although we did not observe effective protection of the striatal tissue *in vitro* by an iNOS inhibitor against thrombin

toxicity (Fujimoto et al., 2006). In this context, Choi et al. (2005) has demonstrated that intrahippocampal injection of thrombin induces microglial activation associated with expression of iNOS and NADPH oxidase, and that resultant increase in oxidative stress contributes to thrombin neurotoxicity.

Overall, we demonstrated that thrombin injected into the striatum caused neuronal damage, which in part involves a delayed phase of neuronal loss with apoptotic features. Prominent activation of microglia exhibiting MAPK activation, as well as a significant protective effect of MAPK inhibitors, suggests that regulation of MAPK pathways and/or microglial activation could be a useful therapeutic intervention against hemorrhagic stroke.

Acknowledgements

This study was supported by Grant-in-aid for Scientific Research from The Ministry of Education, Culture, Sports, Science and Technology, Japan and Japan Society for the Promotion of Science. S. F. is supported as a Research Assistant by 21st Century COE Program “Knowledge Information Infrastructure for Genome Science”.

References

Choi, S.H., Joe, E.H., Kim, S.U., Jin, B.K., 2003. Thrombin-induced microglial activation produces degeneration of nigral dopaminergic neurons in vivo. J. Neurosci. 23, 5877-5886.

Choi, S.H., Lee, D.Y., Kim, S.U., Jin, B.K., 2005. Thrombin-induced oxidative stress contributes to the death of hippocampal neurons in vivo: role of microglial NADPH oxidase. J. Neurosci. 25, 4082-4090.

Donovan, F.M., Pike, C.J., Cotman, C.W., Cunningham, D.D., 1997. Thrombin induces apoptosis in cultured neurons and astrocytes via a pathway requiring tyrosine kinase and RhoA activities. J. Neurosci. 17, 5316-5326.

Fayad, P.B., Awad, I.A., 1998. Surgery for intracerebral hemorrhage. Neurology 51, S69-S73.

Fujimoto, S., Katsuki, H., Kume, T., Akaike, A., 2006. Thrombin-induced delayed injury involves multiple and distinct signaling pathways in the cerebral cortex and the striatum in organotypic slice cultures. Neurobiol. Dis. 22, 130-142.

Gingrich, M.B., Traynelis, S.F., 2000. Serine proteases and brain damage - is there a link? Trends Neurosci. 23, 399-407.

Gong, C., Boulis, N., Qian, J., Turner, D.E., Hoff, J.T., Keep, R.F., 2001. Intracerebral hemorrhage-induced neuronal death. Neurosurgery 48, 875-882.

Huang, F.P., Xi, G., Keep, R.F., Hua, Y., Nemoianu, A., Hoff, J.T., 2002. Brain edema after experimental intracerebral hemorrhage: role of hemoglobin degradation products. J. Neurosurg. 96, 287-293.

Katsuki, H., Okawara, M., Shibata, H., Kume, T., Akaike, A., 2006. Nitric oxide-producing microglia mediate thrombin-induced degeneration of dopaminergic neurons in rat

midbrain slice culture. J. Neurochem. 97, 1232-1242.

Kitaoka, T., Hua, Y., Xi, G., Hoff, J.T., Keep, R.F., 2002. Delayed argatroban treatment reduces edema in a rat model of intracerebral hemorrhage. Stroke 33, 3012-3018.

Koistinaho, M., Koistinaho, J., 2002. Role of p38 and p44/42 mitogen-activated protein kinases in microglia. Glia 40, 175-183.

Lee, K.R., Colon, G.P., Betz, A.L., Keep, R.F., Kim, S., Hoff, J.T., 1996. Edema from intracerebral hemorrhage: the role of thrombin. J. Neurosurg. 84, 91-96.

Matsushita, K., Meng, W., Wang, X., Asahi, M., Asahi, K., Moskowitz, M.A., Lo, E.H., 2000. Evidence for apoptosis after intercerebral hemorrhage in rat striatum. J. Cereb. Blood Flow Metab. 20, 396-404.

Möller, T., Hanisch, U.K., Ransom, B.R., 2000. Thrombin-induced activation of cultured rodent microglia. J. Neurochem. 75, 1539-1547.

Power, C., Henry, S., Del Bigio, M.R., Larsen, P.H., Corbett, D., Imai, Y., Yong, V.W., Peeling, J., 2003. Intracerebral hemorrhage induces macrophage activation and matrix metalloproteinases. Ann. Neurol. 53, 731-742.

Ryu, J., Pyo, H., Jou, I., Joe, E., 2000. Thrombin induces NO release from cultured rat microglia via protein kinase C, mitogen-activated protein kinase, and NF-κB. J. Biol. Chem. 275, 29955-29959.

Sansing, L.H., Kaznatcheeva, E.A., Perkins, C.J., Komaroff, E., Gutman, F.B., Newman, G.C., 2003. Edema after intracerebral hemorrhage: correlations with coagulation parameters and treatment. J. Neurosurg. 98, 985-992.

Sinar, E.J., Mendelow, A.D., Graham, D.I., Teasdale, G.M., 1987. Experimental intracerebral hemorrhage: effects of a temporary mass lesion. J. Neurosurg. 66, 568-576.

Suo, Z., Wu, M., Citron, B.A., Gao, C., Festoff, B.W., 2003. Persistent protease-activated receptor 4 signaling mediates thrombin-induced microglial activation. J. Biol. Chem. 278, 31177-31183.

Weinstein, J.R., Hong, S., Kulman, J.D., Bishop, C., Kuniyoshi, J., Andersen, H., Ransom, B.R., Hanisch, U.K., Möller, T., 2005. Unraveling thrombin's true microglia-activating potential: markedly disparate profiles of pharmaceutical-grade and commercial-grade thrombin preparations. J. Neurochem. 95, 1177-1187.

Xi, G., Reiser, G., Keep, R.F., 2003. The role of thrombin and thrombin receptors in ischemic, hemorrhagic and traumatic brain injury: deleterious or protective? J. Neurochem. 84, 3-9.

Xi, G., Keep, R.F., Hoff, J.T., 2006. Mechanisms of brain injury after intracerebral haemorrhage. Lancet Neurol. 5, 53-63.

Xue, M., Del Bigio, M.R., 2001. Acute tissue damage after injections of thrombin and plasmin into rat striatum. Stroke 32, 2164-2169.

Figure legends

Fig. 1. Thrombin-induced neuronal death and nuclear fragmentation. Brains were transcardially fixed by 4% paraformaldehyde, and coronal cryosections were prepared. Shown are representative images of coronal sections immunostained with anti-NeuN antibody at low (A, D, G and J) and high (B, E, H and K) magnification and Hoechst 33342-stained sections (C, F, I and L). The sections were prepared from brains at 72 h after saline injection (A-C), 4 h (D-F), 24 h (G-I) and 72 h (J-L) after thrombin injection. Arrowheads in I and L indicate fragmented nuclei. Scale bars, 1 mm (A, D, G and J), 100 μm (B, E, H and K) and 20 μm (C, F, I and L). (M) The number of NeuN-positive cells at the injection site, at indicated periods after saline and thrombin treatment. n=4-6.

Fig. 2. Representative images of brain coronal sections immunostained with anti-OX42 antibody. Images are of the injection site at 72 h after saline (A), 4 h (B) and 72 h (C) after thrombin injection, and of the contralateral striatum at 72 h after thrombin injection (D). Scale bar, 20 μm.

Fig. 3. Effects of MAPK inhibitors administered by intrastriatal injection concomitant with thrombin. (A-D) Representative images of NeuN-immunostained coronal sections prepared from brains after 72 h of injection of thrombin alone (20 U with DMSO, 1:3; A), thrombin plus PD98059 (5 nmol; B), SB203580 (5 nmol; C) and SP600125 (5 nmol; D). Scale bar, 1 mm. (E) The degree of injury was determined by the area devoid of NeuN immunoreactivity in the striatum. Vehicle (veh, DMSO diluted 1:3 with saline) was also injected as control. # $P < 0.001$ vs. vehicle, * $P < 0.05$ vs. thrombin alone, n=7-9.

Fig. 4. Thrombin-induced phosphorylation of ERK and p38 MAPK. (A) Representative immunoblots showing ERK and p38 MAPK phosphorylation in response to thrombin. After indicated periods of injection, homogenates were prepared from 2 mm-thick sections of ipsilateral (i) and contralateral (c) striatum containing the injection site, and lysates were subjected to western blot analysis with specific antibodies against phosphorylated ERK, total ERK, phosphorylated p38 MAPK, total p38 MAPK and β-actin. (B) Time course of ERK phosphorylation. Ratio of phosphorylated ERK vs. total ERK at each time point was calculated. * $P < 0.05$ vs. saline (4 h), n=3. (C) Time course of p38 upregulation. Ratio of total p38 MAPK vs. β-actin at each time point was calculated (n=3). (D) Confocal immunofluorescence images of phosphorylated ERK (left) and OX42 (center), and their merged image (right) after 4 h of thrombin injection. (E) Confocal immunofluorescence images of phosphorylated p38 MAPK (left) and OX42 (center), and their merged image (right) after 72 h of thrombin injection. Arrowheads in D and E indicate colocalization. Scale car, 20 μm.

Fig. 5. Involvement of activated microglia in thrombin neurotoxicity. (A, B) Effect of minocycline (MINO) on the number of activated microglia at the injection site (A) and the area injured by thrombin (B). MINO was intraperitoneally administered at a dose of 45 mg/kg at 1 and 13 h after thrombin injection and 22.5 mg/kg at 25, 37 and 49 h. n=5. (C, D) Confocal immunofluorescence images of iNOS (red) and OX42 (green) at the ipsilateral (C) and the contralateral (D) striatum after 24 h of thrombin injection. Arrowheads indicate iNOS-positive microglia. Scale car, 10 μm.

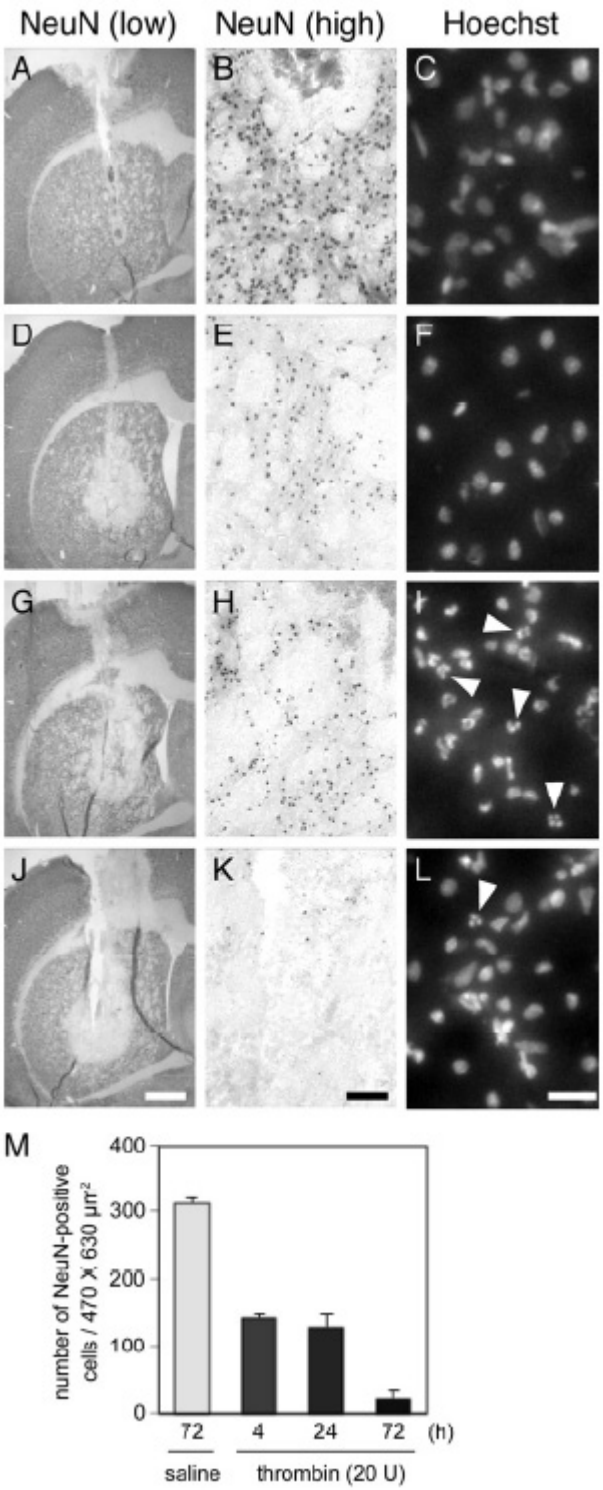
NeuN (low)
NeuN (high)
Hoechst
A
B
C
D
E
F
G
H
I
J
K
L
M
number of NeuN-positive cells / 470 X 630 μm²
400
300
200
100
0
72
4
24
72
(h)
saline
thrombin (20 U)

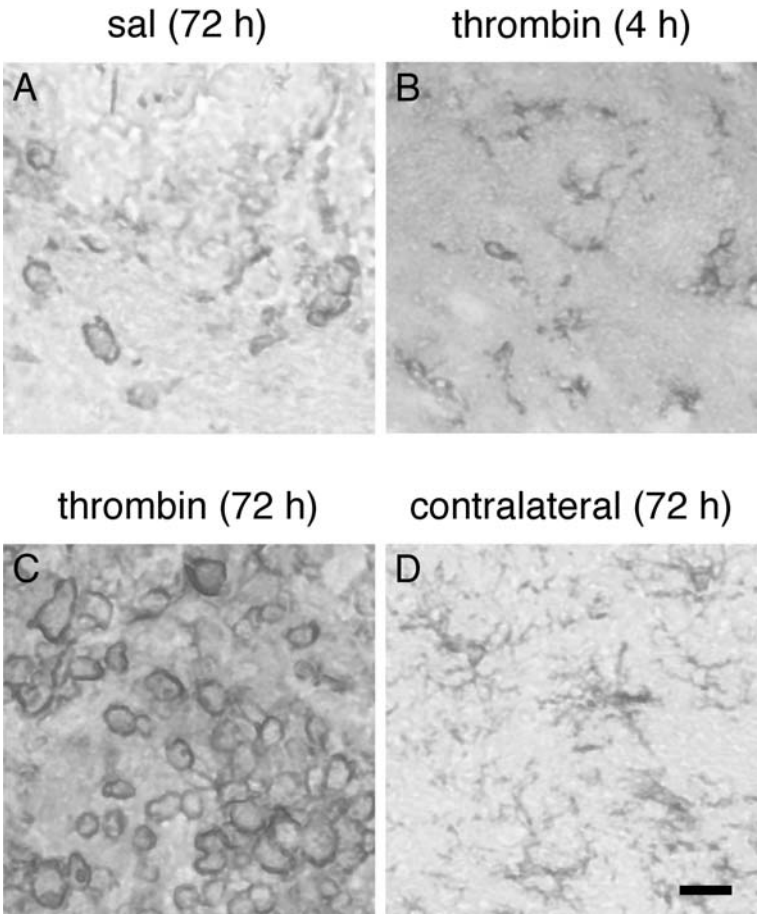
sal (72 h)
thrombin (4 h)
A
B
thrombin (72 h)
contralateral (72 h)
C
D

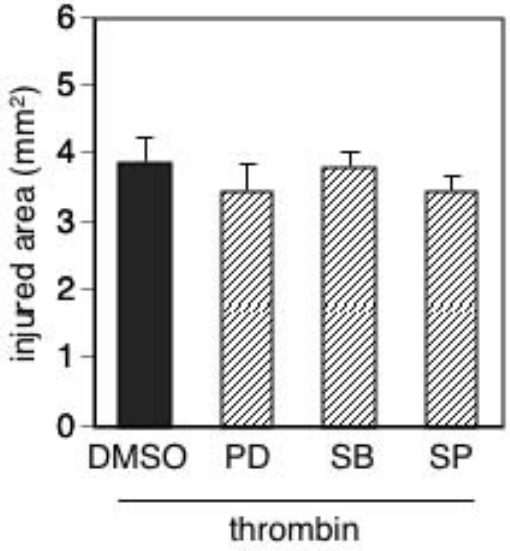
injured area (mm²)
6
5
4
3
2
1
0
DMSO
PD
SB
SP
thrombin

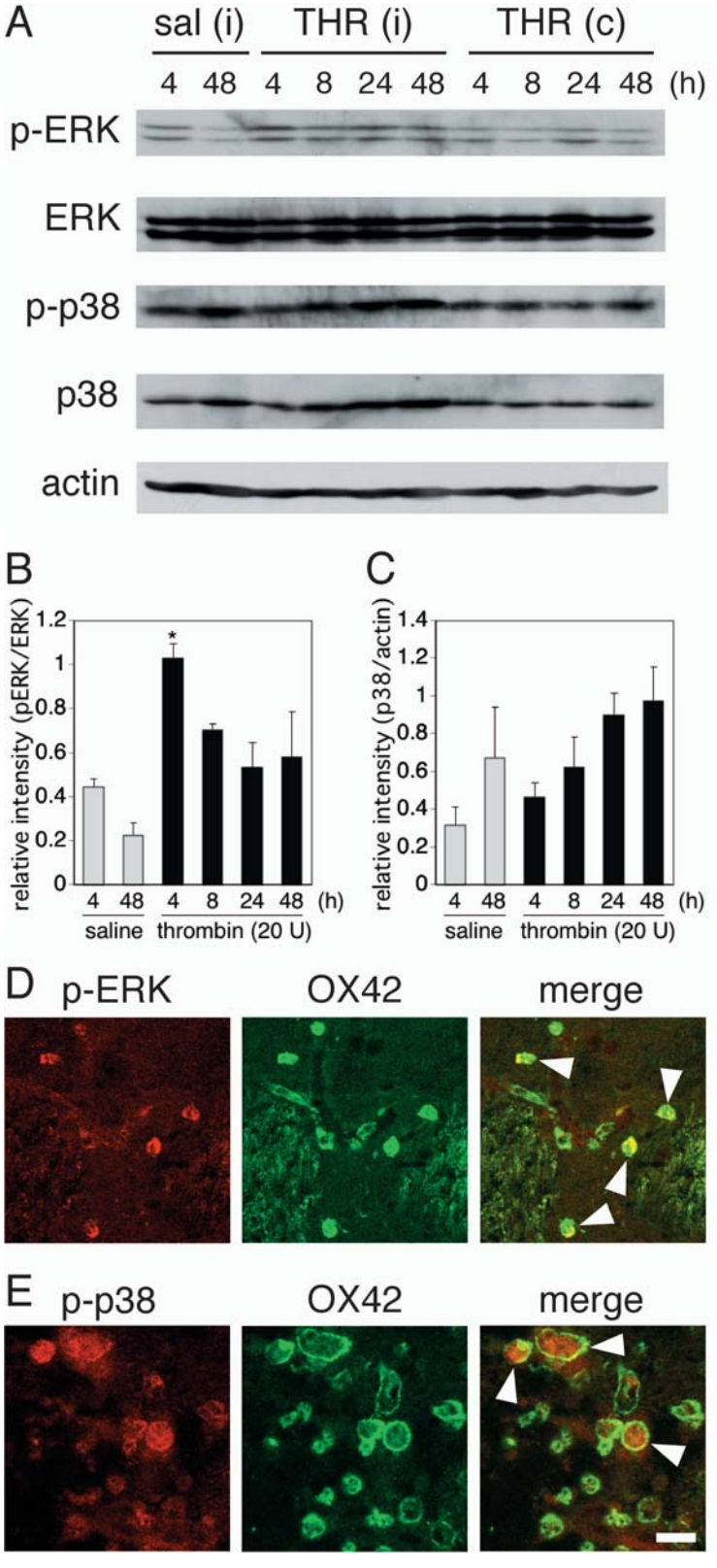
A
sal (i)
THR (i)
THR (c)
4 48 4 8 24 48 4 8 24 48 (h)
p-ERK
ERK
p-p38
p38
actin
B
relative intensity (pERK/ERK)
1.2
1
0.8
0.6
0.4
0.2
0
*
4 48 4 8 24 48 (h)
saline
thrombin (20 U)
C
relative intensity (p38/actin)
1.4
1.2
1
0.8
0.6
0.4
0.2
0
4 48 4 8 24 48 (h)
saline
thrombin (20 U)
D
p-ERK
OX42
merge
E
p-p38
OX42
merge

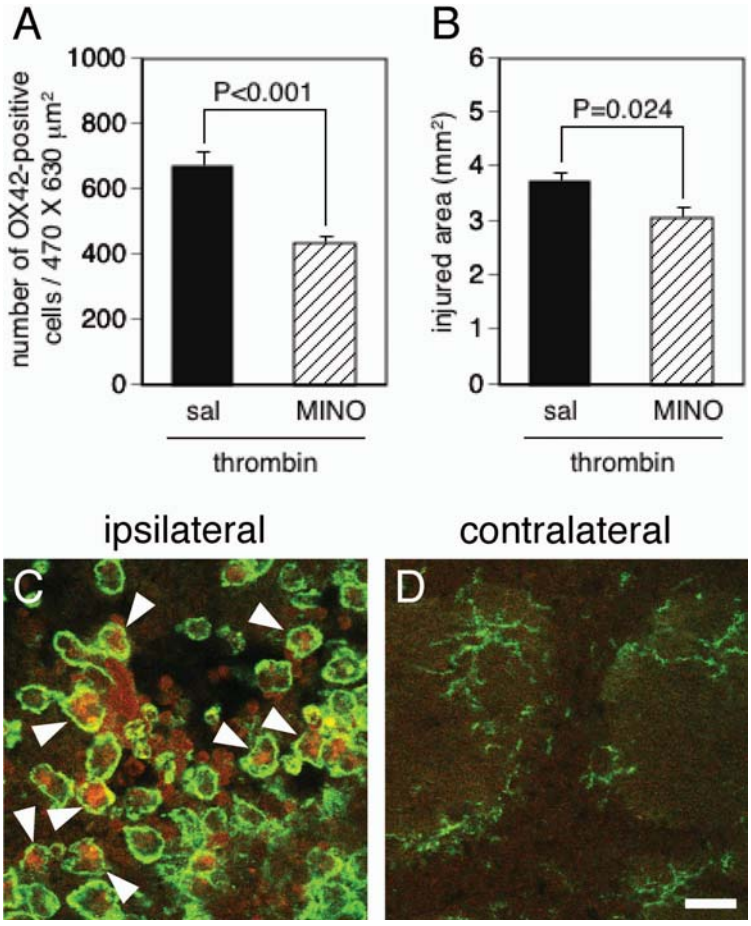
A
number of OX42-positive cells / 470 X 630 μm²
1000
800
600
400
200
0
P<0.001
sal
MINO
thrombin
B
injured area (mm²)
6
5
4
3
2
1
0
P=0.024
sal
MINO
thrombin
ipsilateral
contralateral
C
D